American Mineralogist, Volume 61, pages 839–852, 1976

Proudite from Tennant Creek, Northern Territory, Australia: its crystal structure and relationship with weibullite and wittite

WILLIAM G. MUMME

CSIRO Division of Mineral Chemistry
P.O. Box 124, Port Melbourne, Victoria 3207, Australia

Abstract

Proudite, from the Juno Mine at Tennant Creek, Northern Territory, Australia, is monoclinic, space group $C2/m$, with $a = 31.96(1)$, $b = 4.12(1)$, $c = 36.69(3)$ Å, $\beta = 109.52(3)°$ and has a known range of solid solution expressed by the general formula $Cu_xPb_{7.5}Bi_{9.67-0.33x}(S_y, Se_{1-y})_{22}$, where $0.04 < x < 0.98$ and $0.57 < y < 0.82$. Single-crystal X-ray data were collected using the integrating Weissenberg equi-inclination method with multiple film packs; and the structure was solved by the Patterson method and refined by a least-squares procedure to give a final R of 0.17. The asymmetric unit contains 8 Pb, 10 Bi, 1 Cu, and 23 S atom sites. The Cu site, one Bi, and two S sites are partially occupied and the solid solution $Pb_{7.5}Bi_{9.67}(S,Se)_{22} \rightleftarrows CuPb_{7.5}Bi_{9.33}(S,Se)_{22}$ probably exists. Pb and Bi atoms may be distinguished with only a moderate degree of confidence on the basis of differences in their bonding geometry; the selenium is preferentially ordered into seven of the anion lattice sites. The structure of proudite is closely related to that of junoite, $Cu_2Pb_3Bi_8(S,Se)_{16}$, the other main selenium-rich mineral intergrown with proudite at Juno. This study also incorporates new X-ray and chemical data on the little studied seleniferous sulphosalts wittite and weibullite, and proves that all three are distinct mineral species. Zoning of bismuth-rich sulphosalts in the ore bodies at Juno is discussed.

Introduction

Selenium substitutes for sulphur in many sulphide and sulphosalt minerals, so that distinct Se minerals rarely occur in massive sulphide deposits. Sulphides and selenides are present together because they have formed either at different periods of mineralization or at times when the mineralizing solutions were considerably deficient in S. In contrast to sulphur, which under natural conditions forms compounds of one type or another with at least 40 chemical elements, selenium does so with just a few of higher atomic number. Selenium compounds with light metals do not exist in nature, and there is a predominance of selenides of copper, silver, and bismuth, and notably a lack of compounds with gold which is so specific for its analog tellurium (Sindeeva, 1964).

Although relatively few selenium minerals have been reported as distinct species, there are many descriptions of selenium-bearing minerals in the literature. Sulphur–selenium isomorphism in them is extensive and often unlimited, as is illustrated both in synthetic compounds and in natural specimens, *e.g.* the solid solutions PbS–PbSe and Bi_2S_3–Bi_2Se_3 (Earley, 1950), where 1:1 replacement of S by Se is possible. In particular, the selenide minerals of lead and bismuth included in this type are clausthalite, PbSe, isomorphous with galena; guanajuatite, $Bi_2(S,Se)_3$, isomorphous with bismuthinite; and paraguanajuatite, Bi_2Se_3, which has a structure analogous to tetradymite (Bi_2Te_2S). Other reported occurrences of somewhat more complex lead–bismuth sulphosalts which also fall into this category of sulphur–selenium isomorphism are laitakarite, Bi_4SSe_2, (Vorma, 1960); selenocosalite (Ödman, 1941); selenolillianite, $Pb_3Bi_2(S,Se)_6$, and selenogoongarite, $Pb_4Bi_2(S,Se)_7$ (by Isaksson; see Grip and Wirstam, 1970). These occurrences, at Orijarvi, Finland, and the Boliden Mine, Sweden, must be regarded as somewhat doubtful, particularly selenocosalite which appears to have the wrong composition for it to be a Se-isomorph of cosalite, and selenogoongarite for the reason that goongarite itself is a discredited mineral. Laitakarite and ikunolite, $Bi_4(S,Se)_3$ (Kato, 1959), are reported to be isostructural with joseite-A, $Bi_{4+x}Te_{1-x}S_2$.

Many of the early described selenium-bearing minerals were found to be mixtures in later investigations, and this has left some doubt concerning the few remaining species. Thus, the little-studied minerals wittite, weibullite, and platynite were until recently the only lead–bismuth sulphosalts which could in any way be regarded as distinct seleniferous sulphosalts because, if valid species, they probably could not form without the presence of selenium. These three minerals were found at Falun, Sweden, an old mining district where massive pyrite carried copper mineralization, and they were the subject of investigations by Swedish mineralogists in the late 1800's and early 1900's.

The discovery of seleniferous bismuth sulphosalts in the Juno Mine, Tennant Creek, Northern Territory, Australia (Large, 1974; and Large and Mumme, 1975), added several new species to this rather small group of minerals. One of the new minerals, junoite [$Cu_2Pb_3Bi_8(S,Se)_{16}$] has up to 11.4 percent Se, partially ordered into two of the sulphur sites in its structure (Mumme, 1975a). The other main lead–bismuth mineral in the deposit, now named proudite, was reported as having a composition close to $Bi_{10}Pb_8(S,Se)_{23}$ [in Large and Mumme (1975) it was referred to as "wittite"] and contains from 6.5 to 15.3 weight percent Se, representing a maximum of 9 selenium atoms in the above formula unit. Like junoite, it is one of a unique group of minerals, and knowledge of its crystal structure is important in order to relate it both to junoite and other seleniferous varieties of lead–bismuth sulphosalts.

Previous studies of selenium-bearing bismuth–lead sulphosalts

Weibullite was first described by Nordström (1874), Atteberg (1874), and Weibull (1885). Johansson's studies (in the 1920's) were later summarized by Wickman (1948). The chemical analysis and X-ray data given in Johansson's notes indicate that he considered the material was identical with selenium-bearing galenobismutite. This result was not confirmed in later studies by Peacock and Berry (1940), who identified two minerals in the specimens. The major of these they indicated was monoclinic with $a = 18.03$, $b = 4.04$, $c = 17.53$ Å, and $\beta = 94.29°$, the other phase was hexagonal with $a = 4.20$ and $c = 13.22$ Å. These two minerals were referred to as weibullite and selenjoseite respectively by Berry and Thompson (1962). They stated that samples from Falun labelled as weibullite, galenobismutite, and seleniferous chiviatite all showed this same intimate mixture of weibullite, selenjoseite, and bismuthinite, and therefore concluded that Johansson's analyses were based on mixtures.

More recently Karup-Møller (1970a) carried out a study of specimen BSF 1753, labelled "weibullite from Falun grufva" from the mineralogical collection at Bergskolan in Filipstad, Sweden. This study of weibullite, selenjoseite, and bismuthinite placed particular emphasis on the chemical composition of these minerals using microprobe analysis. Selenjoseite was found to be identical with laitakarite (Vorma, 1960). Weibullite, identified from the powder pattern given by Berry and Thompson (1962), was found to have a composition close to $Bi_6Pb_4S_9Se_4$.

Platynite, also from Falun, was first described by Flink (1910). His reported analysis (Cu 0.32, Fe 0.30, Pb 25.80, Bi 48.98, S 4.36, Se 18.73%), performed by Mauzelius, suggests the formula $Pb_4Bi_7S_4Se_7$. Later an occurrence of platynite was described by Babkin (1958) in one of the tin ore deposits in northeastern USSR. The analysis of this material showed wide variations in the contents of the various components (Pb 14.81–7.0, Bi 65.63–55.23, S 11.74–7.49, and Se 18.24–9.76%). According to Vlasov (1964, p. 672), Godovikov and Fer'yanchich later identified this material as laitakarite (Vlasov suggests that Flink's platynite was a mixture).

Wittite from Falun was named by Johansson (1924). His analyses gave Pb 33.85, Bi 43.33, S 12.14, Se 8.46, Ag 0.19, Zn 0.26, Cu 0.08, Fe 0.28, insoluble residue 0.54, total 99.13 percent. Strunz (1957) has regarded this mineral as Se-rich hammarite, as does Povarennykh (1972), although there did not appear to be enough copper reported in the analyses for this to be the case. Alternative interpretations have suggested that Johansson's specimen was an intergrowth of two minerals (Sindeeva, 1964).

Argentiferous wittite has also been reported in the sulphidic wolframite ores of the lower horizons of the Belukhinsk deposits (Eastern Trans-Baikal) by Ontoev *et al.* (1972). Their analysis (average of three) gave Bi 47.9, As 0.6, Pb 30.3, Ag 5.15, Se 0.15, and S 16.0 percent. They also reported the X-ray powder data reproduced here in Table 1, where it is compared with X-ray patterns of gustavite, $Bi_{11}Pb_5Ag_3S_{24}$, and phase *X*, $Bi_{10}Pb_7Ag_2S_{24}$, which are Ag-containing members of the lillianite ($Pb_3Bi_2S_6$)–$AgPbBi_3S_6$ system (Karup-Møller, 1970b). It appears from both the chemical data (Fig. 1a) and these X-ray data, that the Ag–wittite described by Ontoev *et al.* is most likely a member of the lillianite–$AgPbBi_3S_6$ system, which

TABLE 1A. X-ray powder data for Ag-wittite and gustavite, phase *X* mixture

Gustavite, phase X		Ag-Wittite	
I	d	I	d
1	9.846		
2	6.381		
2*	6.130		
1*	5.806		
1	5.565		
1	4.705		
5	3.977		
2	3.844		
3*	3.721	1	3.743
8	3.640	3	3.625
3	3.592		
1	3.551		
3*	3.516		
2*	3.509(?)		
3†	3.477	2	3.493
8	3.401		
8	3.376	10	3.381
10	3.363		
5	3.326		
4*	3.304		
2*	3.282		
1	3.237	1	3.257
3	3.190	1	3.195
3	3.068		
2	3.033		
10	2.996	6	2.990
4*	2.953		
4	2.911		
10	2.895	9	2.895
2*	2.804		
8	2.751	3	2.753
		1	2.336
		1	2.258
		4	2.13
		1	2.084
		8	2.043
		2	1.958
		3	1.746
		1	1.668
		1	1.446
		1	1.410

* *Lines caused by superstructure of lattice*

† *Line due to phase X*

TABLE 1B. Electron probe analyses for Ag-wittite, gustavite, and phase *X*

	Ag-Wittite	Gustavite	Phase X
Ag	5.15	7.39	4.33
Pb	30.3	22.82	32.17
Bi	47.9	51.15	44.95
S	16.0	17.13	16.60
Se	0.15		

alone tends to leave wittite in the same doubtful status it had before this Russian occurrence was reported.

The wittite, weibullite, proudite problem

When proudite with a composition close to $Bi_{10}Pb_8(S,Se)_{23}$ was discovered at Juno it was extremely difficult to distinguish from weibullite and wittite because of their similar compositions (Table 2 and Fig. 1b) and the limited X-ray data available for weibullite and wittite. Therefore, a specimen of weibullite was obtained from Dr. Karup-Møller, and X-ray powder patterns and single crystal data were recorded for it. These are presented in Table 3, where it is seen that the powder data agreed with the results of Berry and Thompson (1962), though the unit cell and symmetry were completely different. Karup-Møller's chemical data and the X-ray data determined in our laboratories confirmed that weibullite is a unique mineral species, not the same as the Juno Mine mineral.

At this stage the problem still remained as to whether the mineral from Juno was the same as wittite, or whether wittite itself was a mixture of minerals as suggested by Sindeeva. A small specimen of wittite was obtained from the collections of the Naturhistoriska Riksmusseet, Stockholm. A photograph of this specimen is shown in Figure 2. As the mineral is so rare only small fragments have been removed for the purpose of obtaining single-crystal Weissenberg, Guinier X-ray powder diffraction, and electron probe analysis data.

The electron probe analysis gave the following result: Pb 35.3, Bi 43.9, Se 7.7, S 12.6, total 99.5 percent, which agreed well with the previously reported chemical analysis for wittite (see Table 2). The X-ray powder and single-crystal data (Table 4) proved wittite to be a different species from both weibullite and the Juno mineral; the single-crystal data cannot yet be fully evaluated due to the poor quality of the crystals so far investigated, but it indicates wittite is monoclinic with a 4 Å repeat axis and a strong subcell, $a = 29.15$, $b = 4.07$, $c = 15.83$ Å, $\beta = 98.5°$. Status for the Juno mineral to be recognized as a distinct species was then sought from the IMA and proudite suggested as a suitable name. Hence forward we shall refer to this mineral, ideally $CuPb_{7.5}Bi_{9.33}(S,Se)_{22}$, as proudite.

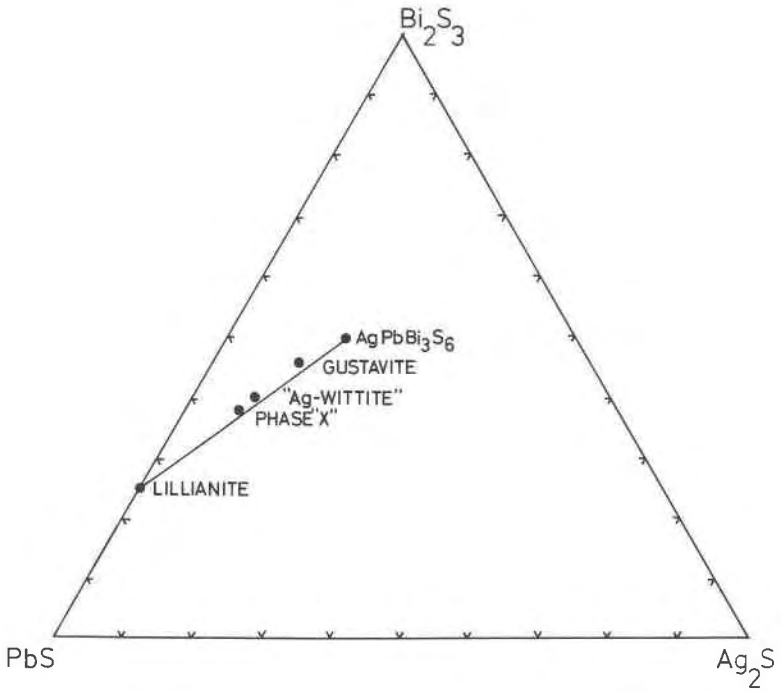

FIG. 1A. Known minerals of the lillianite–$AgPbBi_3S_6$ series, showing their relationship with "Ag-wittite" (Ontoev *et al.*, 1972).

Experimental

Crystals of proudite were isolated from specimen R27789, University of New England collection (Large and Mumme, 1975). The precise unit cell parameters $a = 31.96 \pm .01$, $b = 4.12 \pm .01$, $c = 36.69 \pm .03$Å, $\beta = 109.52 \pm .03°$, ρ calc = 7.08 gm/cm^3, were obtained by refining Guinier X-ray data (Table 5), internally calibrated with KCl ($a_0 = 6.2929$Å), indexed with the aid of Weissenberg films.

TABLE 2. Microprobe and chemical analyses of weibullite, wittite, and proudite

	Proudite			Weibullite	Wittite	
	(1)	(2)	(3)	(4)	Johansson (5)	Microprobe (6)
Bi	42.39	42.7	43.3	47.5	43.33	43.9
Pb	33.78	33.0	33.7	30.8	33.85	35.3
Cu	1.38	1.0	0.5	0.1	0.08	
S	10.43	10.7	9.9	10.3	12.14	12.6
Se	12.02	12.8	14.0	11.6	8.46	7.7
Ag	-			0.8	0.19	
Zn	-				0.26	
Fe	-				0.28	
	100	100.2	101.4	101.1	98.6	99.5

(1) *Ideal proudite,* $CuPb_{7\frac{1}{2}}Bi_{9-1/3}S_{15}Se_7$.
(2) *Average of four analyses of R27789.*
(3) *Average of eleven analyses of proudite.*
(4) *Data from Karup-Møller (1970a), average of three analyses.*
(5) *Johansson's (1924) analysis.*
(6) *Microprobe analysis determiend in these laboratories.*

The systematic absences of the $h0l$, $h1l$ and $h2l$ Weissenberg films recorded about the short 4Å axis, namely hkl, $h + k \neq 2n + 1$; $h0l$, $h \neq 2n$ defined the space group possibilities as $C2/m$, Cm, or $C2$. The reflections with $k = 0, 2$ showed nearly the same intensity distribution, which indicated strongly that almost all of the atoms in this structure are in planes which are normal to the b axis, separated by one-half of the repeat distance of 4Å. Therefore it was assumed that the centrosymmetric space group $C2/m$ is the most probable, a choice which was later confirmed by the satisfactory solution and refinement of the structure.

Intensities, measured visually using a calibrated film strip, were collected using a Weissenberg camera, multiple film packs and Cu$K\alpha$ radiation, from a crystal 0.2 mm long (corresponding to the b direction) and between 0.04 mm and 0.06 mm in average cross section. Absorption factor μR was close to 7, and the approximation used for absorption corrections was that of a cylindrical specimen. Later attempts to use a more sophisticated shape did not result in an improvement of the R value obtained. Considerable difficulty was experienced in obtaining a suitable crystal, as most gave split reflections, and the one finally used, while by no means perfect, was the best of the very many examined.

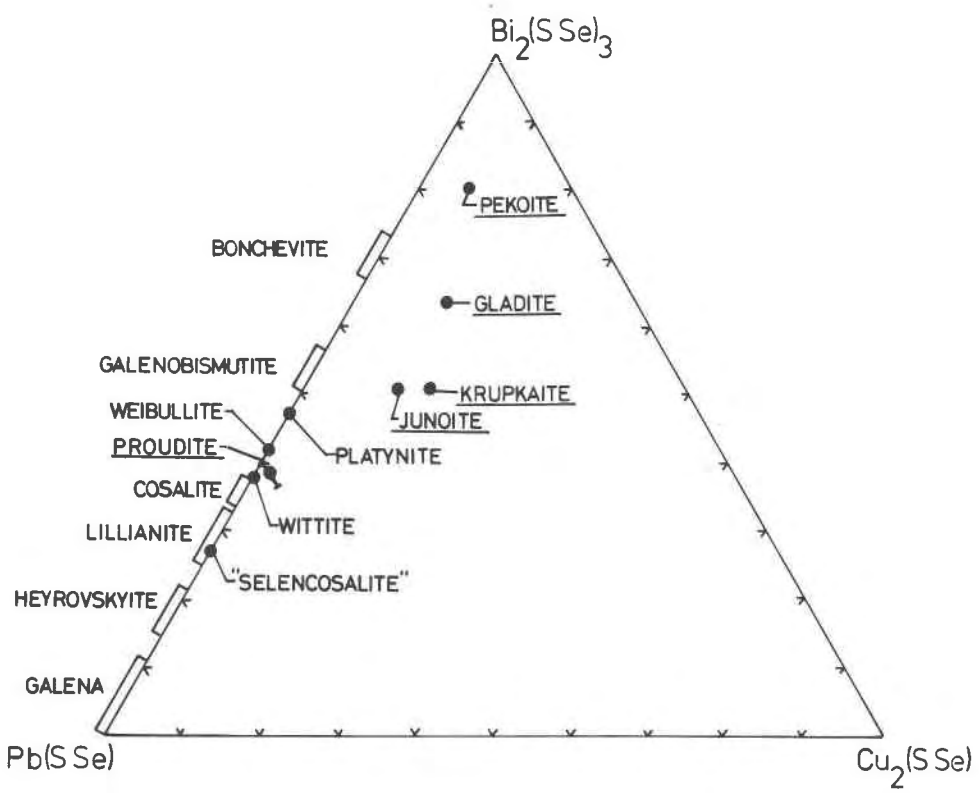

FIG. 1B. Minerals in the system $Bi_2(S,Se)_3$–Pb(S,Se)–$Cu_2(S,Se)$. Those found at Tennant Creek are underlined. They include (a) pekoite [name approved by IMA, July 1975], ideally $CuPbBi_{11}(S,Se)_{18}$ (b) gladite, ideally $CuPbBi_5S_9$ (c) krupkaite [name approved by IMA, June 1974. This redefinition of $CuPbBi_3S_6$ has incorporated a transfer of the name *lindströmite* to the mineral of composition $Cu_3Pb_3Bi_7S_{15}$ (approved by the IMA, September, 1975).], ideally $CuPbBi_3S_6$ (d) junoite, ideally $Cu_2Pb_3Bi_8(S,Se)_{16}$ and (e) proudite, ideally $CuPb_{7.5}Bi_{9.33}(S,Se)_{22}$. Only the solid solution range for proudite is shown.

Structure determination and refinement

The proposed formula, $Bi_{10}Pb_8(S,Se)_{23}$, for proudite had been deduced from the compositions determined by electron probe analysis (Large and Mumme, 1975). It was also based on the unit-cell volume, calculated density, and the space-group requirements. In such a formula the equivalent of 7–9 of the nonmetal atoms would be selenium, and for some specimens this formula unit would have to contain one copper atom, as the analyzed copper content of proudite varied from less than 0.06 to a maximum of 2 percent. It had been concluded (Large and Mumme, 1975) that the specimens of proudite examined were members of an isomorphous series $(Pb,Bi)_{18}(S,Se)_{23} \rightleftarrows (Pb,Bi)_{17.5}Cu(S,Se)_{23}$, and that the mineral contained a copper site which was sometimes only partially occupied. The average composition determined for the sample from which the single crystal was obtained (R27789), given in Table 2, corresponded to a 75 percent occupancy of this copper site.

The short repeat distance of 4Å allows only the two-fold and four-fold sites at $y = 0$ and $y = \frac{1}{2}$ of the assumed space group to be occupied, and the structure solution was attempted using only the $h0l$ data from which a Patterson function $P(u,0,w)$ was calculated. Although the final solution of the structure showed that one lead atom occupied the origin, this assumption was at various times discarded in favor of other models based on a sulphur or selenium atom occupying the origin. The structure solution was a lengthy one, in which by reiteration of structure-factor and electron-density calculations all the metal atoms and all but three of the sulphur atoms were located using the $h0l$ data. Preliminary bond-length calculations were helpful in assigning y parameters, and these were confirmed by three-dimensional Fourier calculations using the three-dimensional data. These calculations also determined the remaining

TABLE 3. X-ray powder data for weibullite (Cu$K\alpha$)

Guinier data, present study				Berry and Thompson (1962)	
d(obs)	d(calc)	h k ℓ	I	d(obs)	I
				7.56	1
				5.13	2
				4.42	2
4.100	4.121	11.0.2	VW		
3.969	3.973	0.0.1	MS	3.92	1
3.868	3.852	0.0.4	S	3.82	10
	3.842	1.0.4			
	3.867	12.0.2			
3.750	3.719	14.0.1	W		
3.626	3.619	1.1.2	MW		
3.605	3.638	13.0.2	W		
	3.595	2.1.2			
3.538	3.555	3.1.2	W	3.56	2
	3.538	6.0.4			
	3.537	11.0.3			
3.506	3.527	7.1.1	W		
	3.506	8.1.0			
3.409	3.431	14.0.2	W		
3.363	3.362	6.1.2	W	3.34	2
	3.372	12.0.3			
3.303	3.306	9.1.1	W		
3.279	3.277	16.0.1	W		
	3.279	7.1.2			
3.233	3.244	15.0.2	VW		
3.210	3.210	0.1.3	W		
	3.217	13.0.3			
3.188	3.187	2.1.3	MS		
3.145	3.159	3.1.3	VW		
	3.129	10.0.4			
3.080	3.072	14.0.3	VS	3.05	9
	3.075	16.0.2			
3.025	3.027	12.1.0	VW		
3.011	3.021	6.1.3	WM		
2.967	2.961	7.1.3	M(B)		
2.898	2.895	8.1.3	M(B)	2.88	3
	2.921	17.0.2			
2.868	2.859	7.0.5	M		
	2.862	13.1.1			
2.811	2.804	14.1.0	W		
	2.808	16.0.3			
2.703	2.689	17.0.3	W	2.71	2
2.689	2.682	6.1.4	WM		
2.648	2.635	14.1.2	VW		
	2.643	20.0.1			
2.563	2.565	1.0.6	VW	2.56	2
2.543	2.556	2.0.6	VW		
	2.542	3.0.6			
	2.543	9.1.4			
2.412	2.401	14.0.5	VW		
2.317	2.314	8.1.5	VW		
	2.316	10.0.6			
2.248	2.241	10.1.5	M	2.24	5
2.109	2.116	6.1.6	M(B)	2.10	1
	2.117	18.1.5			
	2.098	22.1.0			
2.068	2.074	14.1.5	VW		
2.053	2.056	0.2.0	S(B)	2.04	6
	2.046	9.1.6			
	2.064	26.0.0			

Unit Cell: a = 53.68 Å,
b = 4.11(1),
c = 15.40(2).
Space Group Pnma

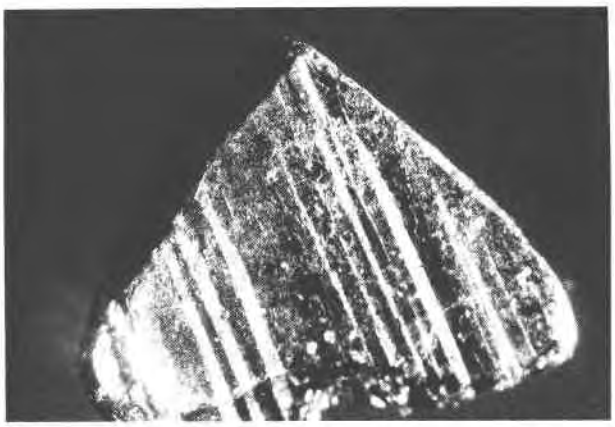

FIG. 2. Photograph of wittite specimen from Naturhistoriska Riksmusseet, Stockholm, made available by Dr. Åberg of that institution. The width of the fragment is 2.5 mm. The *b* axis is parallel to striations seen in the crystal surface.

TABLE 4. Guinier X-ray powder data for wittite from Falun, using Cu$K\alpha$

I	d(meas)	d(calc)	h k ℓ
VW	4.085	4.12	7.0.0
W	3.955	3.91	0.0.4
M	3.848	3.89	$\bar{7}$.0.2
		3.85	$\bar{7}$.0.1
W	3.788	3.83	$\bar{3}$.0.4
M	3.607	3.60	8.0.0
		3.63	$\bar{8}$.0.1
M	3.529	3.54	4.1.0
MS	3.434	3.47	$\bar{8}$.0.2
		3.45	3.0.4
		3.44	7.0.2
M	3.390	3.40	8.0.1
WM	3.362	3.40	4.1.1
W	3.297	3.32	$\bar{4}$.1.2
M	3.138	3.12	$\bar{3}$.0.5
		3.14	4.1.2
M	3.058	3.10	8.0.2
M	3.038	3.07	$\bar{5}$.0.4
S	3.004	3.04	$\bar{4}$.1.3
S(B)	2.887	2.90	7.1.0
		2.87	$\bar{8}$.0.4
		2.90	$\bar{7}$.1.1
M(B)	2.849	2.85	3.0.5
		2.84	4.1.3
M(B)	2.800	2.79	$\bar{3}$.1.4
		2.80	7.1.1
		2.78	8.0.3
WM	2.700	2.73	$\bar{4}$.1.4
W(B)	2.103	2.09	$\bar{12}$.1.1
		2.10	$\bar{10}$.0.6
		2.10	$\bar{7}$.0.7
		2.10	$\bar{6}$.1.6
S	2.041	2.05	$\bar{7}$.1.6
		2.04	0.2.0

Unit cell ("sub-cell" only): a = 29.15(9) Å,
b = 4.07(1),
c = 15.83(5),
β = 98.5(2)°.

three sulphur atoms. Positions were refined using a least-squares refinement version of ORFLS (Busing *et al.*, 1962) for which the weighting scheme of Cruickshank *et al.* (1961) was used. Neutral atom scattering curves were used (Cromer and Waber, 1965), and anomalous dispersion corrections were made for lead and bismuth. An average scattering curve of f(0.25 Se + 0.75S) was originally used for the nonmetal atoms.

The final weighted R was 0.17 (unweighted R =

TABLE 5. Guinier X-ray powder data for proudite using Cu$K\alpha$[2]

I	d(meas)	d(calc)	hkℓ	I	d(meas)	d(calc)	hkℓ
1	7.934	7.945	4,0,$\bar{2}$	9	3.036	3.049	6,0,7
						3.039	7,1,$\bar{4}$
3	7.592	7.568	4,0,$\bar{3}$	8	3.012	3.009	3,1,6
2	7.079	6.942	4,0,$\bar{4}$	100	2.960	2.958	5,1,$\bar{8}$
		6.896	4,0,1			2.963	6,0,$\bar{12}$
2	5.310	5.296	6,0,$\bar{3}$	35	2.930	2.923	8,0,5
2	5.153	5.153	6,0,$\bar{4}$	38	2.906	2.904	1,1,8
2	4.350	4.322	0,0,8	15	2.870	2.864	1,1,$\bar{9}$
5	4.074	4.077	1,1,$\bar{1}$	22	2.852	2.849	3,1,7
		4.084	1,1,0			2.847	5,1,5
10	3.999	4.015	1,1,$\bar{2}$	3	2.720	2.714	5,1,6
		3.980	4,0,6	24	2.669	2.671	7,1,$\bar{9}$
38	3.901	3.906	1,1,$\bar{3}$	6	2.619	2.619	12,0,$\bar{7}$
		3.899	8,0,$\bar{5}$	5	2.595	2.589	10,0,4
48	3.834	3.842	0,0,9	3	2.567	2.562	5,1,$\bar{11}$
		3.829	2,0,8	1	2.545	2.547	1,1,$\bar{11}$
		3.827	3,1,$\bar{2}$			2.550	3,1,9
2	3.781	3.784	8,0,$\bar{6}$	1½	2.442	2.437	5,1,$\bar{12}$
2	3.655	3.646	2,0,$\bar{10}$			2.446	12,0,1
18	3.635	3.630	1,1,4	2	2.409	2.405	9,1,3
17	3.553	3.540	6,0,5	24	2.345	2.346	8,0,$\bar{15}$
65	3.494	3.491	3,1,3			2.348	11,1,$\bar{2}$
3	3.470	3.458	0,0,10	1½	2.319	2.317	2,0,14
42	3.447	3.449	1,1,5			2.319	11,1,$\bar{1}$
		3.457	2,0,9	1	2.283	2.280	4,0,13
		3.444	5,1,$\bar{3}$			2.281	11,1,0
9	3.390	3.384	3,1,$\bar{6}$			2.282	14,0,$\bar{5}$
27	3.316	3.306	2,0,$\bar{11}$	3	2.262	2.260	7,1,$\bar{13}$
		3.322	4,0,$\bar{11}$	3	2.185	2.184	11,1,2
27	3.291	3.282	6,0,6	5	2.150	2.152	14,0,0
5	3.268	3.263	1,1,6	17½	2.124	2.124	10,0,$\bar{16}$
		3.271	8,0,3	10	2.095	2.096	13,1,$\bar{3}$
48	3.224	3.223	3,1,$\bar{7}$	30	2.077	2.080	6,0,$\bar{13}$
		3.225	5,1,2			2.080	9,1,$\bar{14}$
5	3.179	3.173	3,1,5			2.077	13,1,$\bar{8}$
7	3.090	3.080	1,1,7	60	2.066	2.072	1,1,14
4	3.062	3.058	3,1,$\bar{8}$	86	2.059	2.061	0,2,0
		3.053	4,0,$\bar{12}$			2.062	3,1,13

0.19). This is high, but what must be taken into account are absorption effects due to irregularities of the crystal shape, which would have little effect in a material with a lower absorption coefficient, and the moderate quality of the X-ray data. Attempts made to improve the R value by applying other absorption corrections were without success. As considerable time had already been spent obtaining this crystal, no further effort was made to obtain a better data set. The final atomic positions and isotropic temperature factors are presented in Table 6. The agreement between observed structure factors and those calculated from these parameters are presented in Table 7.[1]

Results of refinement

The asymmetric unit of proudite contains 42 atomic sites: 18 heavy metal atom sites designated

[1] To obtain a copy of this table, order Document AM-76-020 from the Business Office, Mineralogical Society of America, 1909 K Street, N.W., Washington, D.C. 20006. Please remit $1.00 in advance for the microfiche.

[2] Reproduced from *Economic Geology*, 1975, Vol. 70, p. 377.

TABLE 6. Atomic coordinates in proudite

Site	Occupancy	x	y	z	B(Å^2)
M1	½Pb	0.0000	0	0.0000	1.3(0)
M2	Bi	0.0690(9)	½	0.1017(10)	0.04(7)
M3	Pb	0.1324(8)	0	0.1995(10)	0.17(6)
M4	Bi	0.0050(9)	½	0.1894(10)	0.45(7)
M5	Pb	0.0701(9)	0	0.2930(9)	0.42(7)
M6	Pb	0.1303(7)	½	0.3920(10)	0.45(5)
M7	Bi	0.1979(10)	½	0.3073(10)	1.00(9)
M8	Bi	0.2537(7)	0	0.4043(8)	1.02(5)
M9	Bi	0.1874(10)	0	0.4936(10)	1.8(0)
M10	Pb	0.2351(9)	0	0.1398(10)	1.18(7)
M11	Bi	0.4456(9)	½	0.0914(10)	0.94(7)
M12	Pb	0.1289(10)	½	0.0153(10)	1.52(8)
M13	Pb	0.0038(10)	0	0.4134(10)	3.4(0)
M14	Bi	0.2779(10)	0	0.0551(10)	0.60(8)
M15	Bi	0.3787(10)	0	0.3731(10)	0.73(8)
M16	Pb	0.3550(10)	½	0.1806(15)	2.0(0)
M17	Bi	0.4301(10)	½	0.2956(12)	2.84(9)
M18	0.40Bi	0.2946(10)	0	0.2555(18)	4.8(0)
Cu	0.75Cu	0.1200(63)	½	0.4650(69)	4.7(0)
S1	½S	0.0571(40)	½	0.4986(50)	1.29(8)
S2	S	0.3594(16)	½	0.0470(25)	0.83(9)
S3	S	0.3173(30)	0	0.1274(30)	0.64(7)
S4	S	0.0915(21)	0	0.0622(25)	0.80(9)
S5	S	0.0381(26)	0	0.1474(30)	0.16(7)
S6	S	0.1532(30)	½	0.1501(38)	0.42(9)
S7	S	0.1007(32)	½	0.2561(28)	1.01(7)
S8	Se	0.0417(21)	½	0.3406(25)	0.58(8)
S9	Se	0.1683(19)	0	0.3528(22)	0.56(9)
S10	S	0.1083(25)	0	0.4323(25)	0.24(9)
S11	S	0.2252(25)	½	0.4656(25)	2.16(9)
S12	Se	0.3372(24)	0	0.4655(24)	1.30(8)
S13	Se	0.2766(10)	½	0.3623(14)	0.94(6)
S14	Se	0.2184(20)	0	0.2653(24)	0.33(7)
S15	S	0.4683(14)	0	0.0554(12)	1.83(9)
S16	Se	0.4728(16)	½	0.2212(21	0.60(9)
S17	S	0.2175(25)	½	0.0675(29)	2.40(8)
S18	Se	0.4270(16)	0	0.1349(21)	1.22(9)
S19	½S	0.4185(27)	½	0.4668(29)	0.28(9)
S20	S	0.4579(29)	0	0.3577(31)	0.89(8)
S21	S	0.2549(29)	½	0.2171(32)	2.45(7)
S22	S	0.3943(29)	0	0.2500(29)	1.47(7)
S23	S	0.3540(31)	½	0.3194(31)	1.58(8)

$M(1)$ to $M(18)$, 1 copper atom site and 23 sulphur and selenium atom sites, all located in special positions of space group $C2/m$.

The partially occupied sulphur sites S(1) and S(19) are an unusual feature of this complex structure. Somewhat similar behavior has recently been observed by Takeuchi *et al.* (1974) in the high-temperature phase V on the PbS–Bi_2S_3 join, where a sulphur atom splits into two half-atoms which are separated by 0.6Å, as two systems of covalent bonds would seem to occur statistically in the quenched structure. In the present case also, the two sites are too close together for each to be more than about half occupied by sulphur atoms, and the reason for the splitting seems to be an attempt to satisfy the coordination spheres of both $M(13)$ and $M(15)$ (Fig. 3).

The copper atom occupies a site in which it has three neighbors at 2.35 to 2.46Å and a fourth at the longer distance of 2.69Å, to give it a distorted tetrahedral coordination completed by one of the partially occupied sulphur atom sites. Its coordination and the manner in which it fits into the structure are

very similar to the role of the statistical copper atom in the structure of cosalite, recently described by Srikrishnan and Nowacki (1974). However, the fourth sulphur atom which completes the tetrahedron in cosalite, while at the relatively long distance of 2.61Å, is in a fully occupied site.

Bismuth and lead can be distinguished in lead-containing bismuth sulphosalts on the basis of slight differences in the geometry of their coordination polyhedra. The distance of the closest approach of sulphur to lead is seldom less than 2.8Å, while the minimum bismuth–sulphur distances are in the range 2.5–2.6Å. The closest approaches observed in proudite are $M(2)$ [2.69, 2.75(2)]; $M(4)$ [2.62, 2.73(2)]; $M(7)$ [2.65, 2.78(2)]; $M(8)$ [2.75, 2.81(2)]; $M(9)$ [2.69, 2.76(2)]; $M(11)$ [2.69, 2.68(2)]; $M(14)$ [2.53, 2.96(2)]; $M(15)$ [2.77, 2.78(2)]; $M(17)$ [2.84, 2.66(2)]; and $M(18)$ [2.58, 2.58(2)]. Of these $M(8)$ and $M(15)$ are not as easily categorized as Bi as the others, and there may be some disordering of Pb and Bi into one or both of these sites. The nearest approaches of sulphur atoms for the remaining metal sites are $M(1)$ [3.05(2), 3.28(4)]; $M(3)$ [2.96(2), 2.98]; $M(5)$ [2.81(2), 3.04]; $M(6)$ [2.76(2), 2.83]; $M(10)$ [2.81, 3.26(2)]; $M(12)$ [2.84, 3.16(2)]; $M(13)$ [2.93(2), 3.18]; and $M(16)$ [2.82(2), 3.19(2)]; all with the possible exception of $M(6)$ are sufficiently long to indicate that these positions are occupied by lead atoms alone. However, it is recognized that the structure determination is just about at the limits for distinguishing the Pb and Bi polyhedra, and the above conclusions should be treated with some caution, as the Pb–Bi disorder may be more extensive than is presented in this perhaps oversimplified picture.

If the metal atom sites in the structure are determined on the basis of the bonding geometry, as above, when no copper is present in the structure, the ideal composition of proudite would have to be $Pb_{7.5}Bi_{10}(S,Se)_{22.5}$. This is possible only if S(1) and S(19) are each 75 percent occupied (or together have a total occupancy of 150 percent), and is a composition very close to that determined by the microprobe analysis. However, copper is present in specimen R27789, and a site occupancy of 75 percent has to be assumed for it from the microprobe results, as the structure factor calculations were not sensitive enough to determine an occupancy factor for this site. Furthermore it appears that the charge balance in the structure is maintained upon the introduction of this copper, not by the removal of lead, as previously supposed by Large and Mumme (1975) [*i.e.* $Pb_{7.5}Bi_{10}(S,Se)_{22.5} \rightleftarrows CuPb_7Bi_{10}(S,Se)_{22.5}$], but

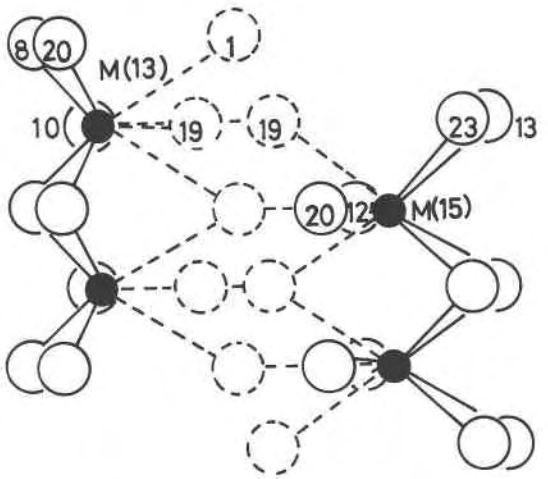

FIG. 3. Coordination polyhedra of atoms $M(13)$ and $M(15)$, showing partially occupied sulphur sites S(1) and S(19).

rather by an adjustment of the bismuth content. This type of behavior is indicated by the final electron density calculations, which showed that one bismuth site, $M(18)$, was only about 50 percent occupied. Consequently there are less than ten bismuth atoms in the formula unit, giving two alternatives for the ideal formula of the copper-rich end member—$CuPb_{7.5}Bi_{9.67}(S,Se)_{22.5}$ or $CuPb_{7.5}Bi_{9.33}(S,Se)_{22}$. The second of these is probably the more likely, as it does not require an occupancy factor greater than 50 percent for the two closely adjacent sulphur sites, S(1) and S(19).

The Fourier analysis indicated that seven of the "sulphur" peaks were considerably higher in electron density than the others. These were therefore regarded as selenium atoms, and refinement was carried out with selenium ordered into these positions. The selenium content for this model (12.02%) is very close to the value determined by microprobe analysis (average = 12.8%), and although it is possible that there is some partial ordering of selenium into other positions, these numerous possibilities were not considered. Selenium has a distinct preference for the sites S(8), S(9), S(12), S(13), S(14), S(16), and S(18), as the R value for the statistically distributed selenium model is 0.19 and that for the ordered model is 0.17.

The ideal composition $CuPb_{7.5}Bi_{9.33}S_{15}Se_8$, deduced for proudite from the structure analysis, is in good agreement with known microprobe analyses for R27789 (Table 2). The known solid-solution range of proudite (Large and Mumme, 1975), together with the structural data, suggests that its composition

TABLE 8. Interatomic distances and bond angles in proudite

Site		Bond Lengths		Bond Angles			
				Bismuth		Lead	
M1	Pb(1)-S(4)	3.05(4)	x2	S(4)-Bi(1)-S(6)	88.1(1)	S(15) -Pb(1)-S(4)	87.3(1)
	S(15)	3.28(5)	x4	S(5)-Bi(1)-S(6)	94.3(1)	S(15)'-Pb(1)-S(4)	92.7(1)
				S(4)-Bi(1)-S(15)	96.7(1)	S(15) -Pb(1)-S(15)'	77.7(1)
M2	Bi(1)-S(6)	2.69(4)		S(5)-Bi(1)-S(15)	80.4(1)	S(15) -Pb(1)-S(15)"	102.3(1)
	S(4)	2.75(4)	x2	S(4)-Bi(1)-S(4)'	97.1(1)		
	S(5)	3.02(5)	x2	S(5)-Bi(1)-S(5)'	85.9(1)	S(6) -Pb(2)-S(14)	99.2(1)
	S(15)	3.10(5)		S(4)-Bi(1)-S(5)	88.5(1)	S(7) -Pb(2)-S(14)	83.4(1)
						S(6) -Pb(2)-S(5)	89.6(1)
M3	Pb(2)-S(6)	2.96(4)	x2	S(5)-Bi(2)-S(7)	88.9(1)	S(7) -Pb(2)-S(5)	86.9(1)
	S(5)	2.98(4)		S(16)-Bi(2)-S(7)	94.2(1)	S(6) -Pb(2)-S(6)'	88.1(1)
	S(14)	2.99(4)		S(18)-Bi(2)-S(5)	91.0(1)	S(7) -Pb(2)-S(7)'	76.9(1)
	S(7)	3.31(5)	x2	S(18)-Bi(2)-S(16)	85.9(1)	S(6) -Pb(2)-S(7)	97.4(1)
				S(5)-Bi(2)-S(5)'	87.8(1)		
M4	Bi(2)-S(18)	2.62(4)		S(16)-Bi(2)-S(16)'	97.9(1)	S(7) -Pb(3)-S(9)	84.9(1)
	S(16)	2.73(4)	x2	S(5)-Bi(2)-S(16)	87.1(1)	S(8) -Pb(3)-S(9)	90.8(1)
	S(5)	2.97(4)	x2			S(7) -Pb(3)-S(16)	90.4(1)
	S(7)	3.22(5)		S(14)-Bi(3)-S(13)	94.8(1)	S(8) -Pb(3)-S(16)	94.3(1)
				S(9)-Bi(3)-S(13)	88.4(1)	S(7) -Pb(3)-S(7)'	94.5(1)
M5	Pb(3)-S(7)	2.81(4)	x2	S(14)-Bi(3)-S(7)	92.2(1)	S(8) -Pb(3)-S(8)'	85.3(1)
	S(8)	3.04(5)		S(9) -Bi(3)-S(7)	84.1(1)	S(7) -Pb(3)-S(8)	89.9(1)
	S(9)	3.20(5)		S(14)-Bi(3)-S(14)'	95.7(1)		
	S(16)	3.33(5)		S(9)-Bi(3)-S(9)'	86.9(1)	S(9) -Pb(4)-S(11)	89.1(1)
				S(14)-Bi(3)-S(9)	88.6(1)	S(10) -Pb(4)-S(11)	83.8(1)
M6	Pb(4)-S(10)	2.76(4)	x2			S(9) -Pb(4)-S(8)	99.0(1)
	S(8)	2.83(4)		S(13)-Bi(4)-S(12)	94.9(1)	S(10) -Pb(4)-S(8)	88.8(1)
	S(9)	2.99(4)	x2	S(11)-Bi(4)-S(12)	82.3(1)	S(9) -Pb(4)-S(9)'	86.9(1)
	S(11)	3.32(5)		S(13)-Bi(4)-S(9)	90.2(1)	S(10) -Pb(4)-S(10)	96.6(1)
				S(11)-Bi(4)-S(9)	91.8(1)	S(9) -Pb(4)-S(10)	87.7(1)
M7	Bi(3)-S(13)	2.65(4)		S(13)-Bi(4)-S(13)'	94.3(1)		
	S(14)	2.78(4)	x2	S(11)-Bi(4)-S(11)'	74.8(1)	S(17) -Pb(5)-S(3)	77.6(1)
	S(9)	3.00(5)	x2	S(13)-Bi(4)-S(11)	95.4(1)	S(21) -Pb(5)-S(3)	102.2(1)
	S(7)	3.04(5)				S(6) -Pb(5)-S(17)	77.3(1)
				S(12)-Bi(5)-S(10)	95.3(1)	S(6)' -Pb(5)-S(17)	122.3(1)
M8	Bi(4)-S(9)	2.75(4)		S(11)-Bi(5)-S(10)	95.3(1)	S(6) -Pb(5)-S(21)	58.8(1)
	S(13)	2.81(4)	x2	S(12)-Bi(5)-S(11)	97.3(1)	S(6)' -Pb(5)-S(21)	102.1(1)
	S(12)	2.86(4)		S(11)-Bi(5)-S(11)"	72.8(1)	S(17) -Pb(5)-S(17)'	78.5(1)
	S(11)	3.39(5)	x2	S(12)-Bi(5)-S(12)'	94.2(1)	S(21)-Pb(5)-S(21)'	74.9(1)
				S(11)-Bi(5)-S(11)'	96.8(1)	S(17)-Pb(5)-S)21)	103.3(1)
M9	Bi(5)-S(11)	2.69(4)		S(12)-Bi(5)-S(11)	83.5(1)		
	S(11)'	2.76(4)	x2				
	S(10)	2.77(4)		S(15)-Bi(6)-S(5)	88.3(1)	S(2) -Pb(6)-S(17)	98.9(1)
	S(12)	2.81(4)	x2	S(18)-Bi(6)-S(5)	87.6(1)	S(4) -Pb(6)-S(17)	96.1(1)
				S(15)-Bi(6)-S(2)	95.3(1)	S(2) -Pb(6)-S(15)	75.1(1)
M10	Pb(5)-S(3)	2.81(4)		S(18)-Bi(6)-S(2)	88.6(1)	S(4) -Pb(6)-S(15)	90.0(1)
	S(17)	3.26(5)	x2	S(15)-Bi(6)-S(15)'	100.8(1)	S(2) -Pb(6)-S(2)'	80.5(1)
	S(21)	3.39(5)	x2	S(18)-Bi(6)-S(18)'	95.2(1)	S(4) -Pb(6)-S(4)'	81.3(1)
	S(6)	3.45(5)	x2	S(15)-Bi(6)-S(18)	81.9(1)	S(2) -Pb(6)-S(4)	97.2(1)
M11	Bi(6)-S(15)	2.68(4)	x2	S(2) -Bi(7)-S(3)	88.0(1)	S(8) -Pb(7)-S(10)	66.6(1)
	S(2)	2.69(4)		S(17)-Bi(7)-S(3)	87.7(1)	S(20)-Pb(7)-S(10)	113.4(1)
	S(18)	2.79(4)	x2	S(2) -Bi(7)-S(2)'	74.3(1)	S(1) -Pb(7)-S(10)	119.3(1)
	S(5)	2.98(4)		S(17)-Bi(7)-S(17)'	88.1(1)	S(20)-Pb(7)-S(19)	94.6(1)
				S(2) -Bi(7)-S(17)	98.6(1)	S(8) -Pb(7)-S(19)	142.0(1)
M12	Pb(6)-S(17)	2.84(4)				S(1) -Pb(7)-S(19)	76.8(1)
	S(4)	3.16(5)	x2	S(23)-Bi(8)-S(20)	85.3(1)	S(20)-Pb(7)-S(20)"	89.5(1)
	S(2)	3.19(5)	x2	S(19)-Bi(8)-S(20)	97.5(1)	S(8) -Pb(7)-S(8)'	64.3(1)
	S(15)	3.32(5)		S(13)-Bi(8)-S(23)	59.2(1)	S(1) -Pb(7)-S(1)'	68.6(1)
				S(13)-Bi(8)-S(19)	79.5(1)	S(20)-Pb(7)-S(8)	95.3(1)
M13	Pb(7)-S(20)	2.93(5)	x2	S(13)'-Bi(8)-S(23)	107.5(1)	S(20)-Pb(7)-S(1)	100.5(1)
	S(10)	3.18(5)		S(13)'-Bi(8)-S(19)	113.8(1)	S(8) -Pb(7)-S(1)	97.2(1)
	S(1)	3.66(5)	x2	S(23) -Bi(8)-S(23)'	95.8(1)		
	S(19)	3.85(5)		S(19) -Bi(8)-S(19)'	64.9(1)	S(18)-Pb(8)-S(16)	58.8(1)
	S(8)	3.87(5)	x2	S(23) -Bi(8)-S(19)	99.7(1)	S(3) -Pb(8)-S(16)	116.0(1)
						S(22)-Pb(8)-S(16)	65.5(1)
M14	Bi(7)-S(3)	2.53(4)		S(22) -Bi(9)-S(23)	87.7(1)	S(18)-Pb(8)-S(21)	146.5(1)
	S(17)	2.96(4)	x2	S(20) -Bi(9)-S(23)	80.4(1)	S(3) -Pb(8)-S(21)	91.6(1)
	S(2)	3.41(5)	x2	S(8) -Bi(9)-S(22)	89.9(1)	S(22)-Pb(8)-S(21)	82.8(1)
				S(8) -Bi(9)-S(20)	47.6(1)	S(3) -Pb(8)-S(3)'	93.9(1)
M15	Bi(8)-S(20)	2.77(4)		S(8)'-Bi(9) -S(22)	143.3(1)	S(18)-Pb(8)-S(18)'	64.4(1)
	S(23)	2.78(4)	x2	S(8)'-Bi(9) -S(20)	92.5(1)	S(22)-Pb(8)-S(22)'	80.5(1)
	S(13)	3.77(5)	x2	S(22)-Bi(9) -S(22)'	101.5(1)	S(3) -Pb(8)-S(18)	59.2(1)
	S(19)	3.84(5)	x2	S(20)-Bi(9) -S(20)'	87.6(1)	S(3) -Pb(8)-S(22)	92.5(1)
				S(22)-Bi(9) -S(20)	84.3(1)	S(18)-Pb(8)-S(22)	82.5(1)
M16	Pb(8)-S(3)	2.82(4)	x2	S(16)-Bi(9) -S(22)	72.7(1)		
	S(22)	3.19(5)	x2	S(16)-Bi(9) -S(20)	120.8(1)		
	S(16)	3.56(5)				Copper	
	S(21)	3.86(5)					
	S(18)	3.86(5)	x2	S(21)-Bi(10)-S(22)	106.2(1)		
				S(23)-Bi(10)-S(22)	72.2(1)	S(10)-Cu-S(10)'	122.4(3)
M17	Bi(9)-S(22)	2.66(4)	x2	S(21)-Bi(10)-S(14)	76.2(1)	S(10)-Cu-S(12)	117.9(3)
	S(23)	2.85(4)		S(23)-Bi(10)-S(14)	104.7(1)	S(12)-Cu-S(1)	76.5(3)
	S(20)	2.98(4)	x2	S(21)-Bi(10)-S(21)'	106.1(1)	S(1) -Cu-S(10)	102.6(3)
	S(16)	3.43(5)		S(23)-Bi(10)-S(23)'	79.5(1)		
				S(21)-Bi(10)-S(23)	87.1(1)		
M18	Bi(10)-S(14)	2.58(4)					
	S(21)	2.58(4)	x2				
	S(23)	3.22(5)	x2				
	S(22)	3.26(5)					
Cu	-S(10)'	2.35(6)					
	S(12)	2.46(6)					
	S(1)	2.69(6)					

may be best expressed by the general formula $Cu_x Pb_{7.5}Bi_{9.67-0.33x}(S_y,Se_{1-y})_{22}$ where $0.04 < x < 0.98$ and $0.57 < y < 0.82$. Bond distances and angles in the structure are presented in Table 8.

Discussion of the structure

The projection of the structure of proudite onto (010) is given in Figure 4. The most significant feature of the structure is the double zig-zag ribbon of edge-shared octahedra, between which are sandwiched further ribbon-like fragments composed of the other bismuth and lead atoms, mostly in 7- and 8-fold coordination, and the tetrahedrally coordinated copper atoms. The double zig-zag ribbon of edge-shared octahedra represents a fragment of galena-like structure which has been observed in many other lead–bismuth sulphides and sulphosalts (Hellner, 1958; Takeuchi and Sadanaga, 1969). The structure of proudite is most closely related to that of junoite, $Cu_2Pb_3Bi_8(S,Se)_{16}$ (Mumme, 1975a), in that both contain similar groupings of PbS-like fragments. In junoite a single extended zig-zag ribbon of the PbS-type has formed, while in proudite the ribbon has double width.

The extent of the PbS fragment which occurs in a particular lead–bismuth sulphosalt depends on the lead:bismuth ratio in the mineral (Hellner, 1958; Takeuchi and Sadanaga, 1969; Kohatsu and Wuensch, 1973; Mumme, 1975a). Those with a high lead content generally have structures with more extensive regions of PbS-like fragments, while those with high Bi content tend to be composed of discrete chains related to the structures of bismuthinite and bismuthinite derivatives (Mumme *et al.*, 1975). Proudite follows this trend in behavior, but the relationship is not straightforward; although proudite

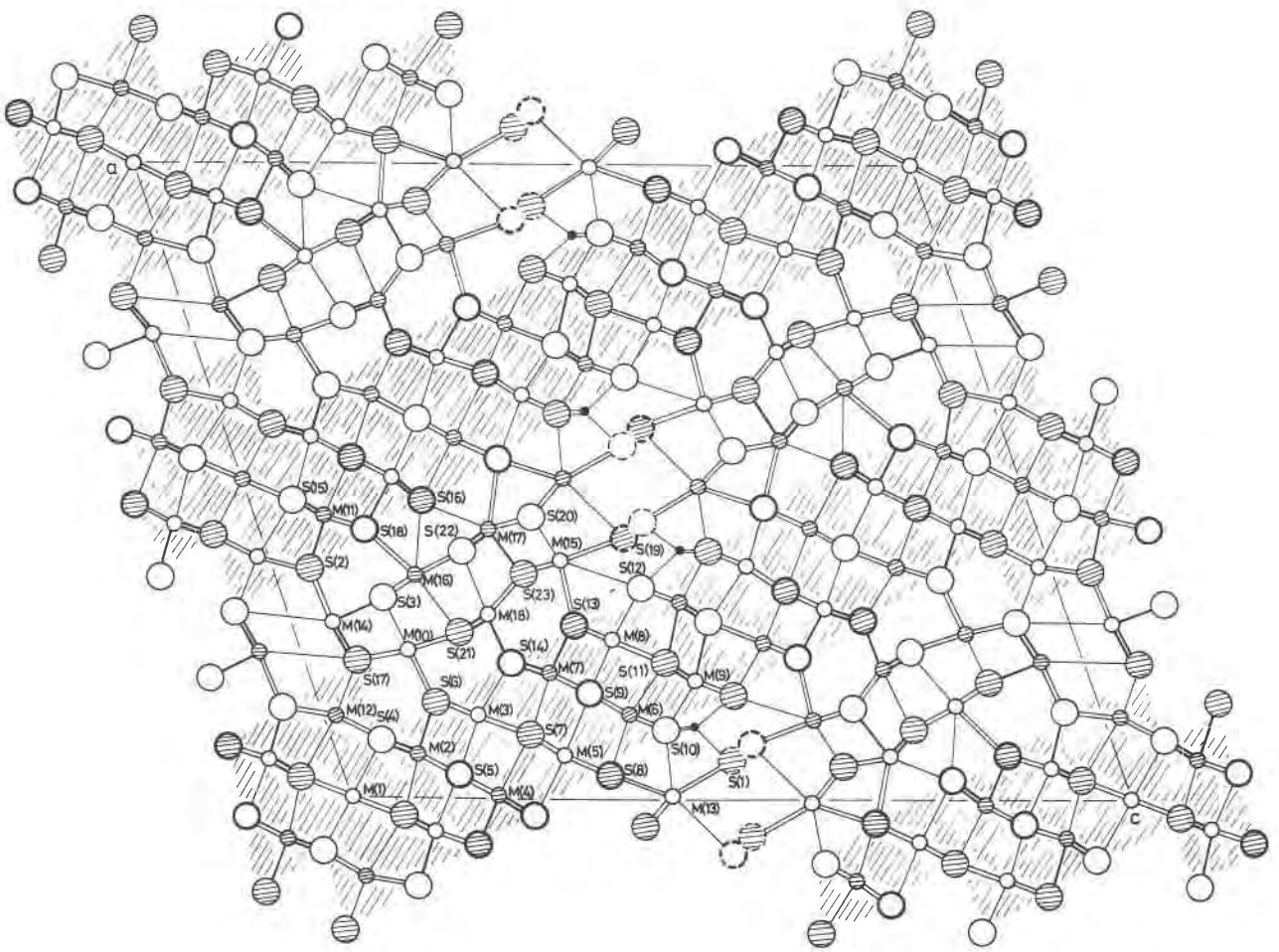

FIG. 4. Proudite as an assemblage of octahedra and other coordination polyhedra. The shaded portions are equivalent to fragments of the PbS type. Hatched circles are at ½, open circles at 0. Medium circles Pb,Bi; large circles S; Se atoms have heavy outlines.

TABLE 9. Lead-bismuth sulphosalts containing PbS-type fragments in their structures

Mineral	Pb/Bi molar ratio	Fraction PbS-type
Galenobismutite $PbBi_2S_4$	0.50	0.30
Cosalite $Pb_2Bi_2S_5$	1.00	0.61
Kobellite $12PbS.7(Bi_{0.56}S_{0.44})S-2(Cu_{0.56}Fe_{0.44})S$	1.70	0.31
Junoite $Cu_2Pb_3Bi_8(S,Se)_{16}$	0.38	0.47
Lillianite $Pb_3Bi_2S_6$	1.50	0.68
Proudite $CuPb_{7\frac{1}{2}}Bi_{9-1/3}(S,Se)_{22}$	0.80	0.45
Hodrushite $PbCu_4Bi_5S_{11}$	0.20	0.19

has a much higher lead/bismuth ratio (0.80) than junoite (0.375), the results in Table 9 show that the relative extents of the PbS fragments are nearly the same in each structure.

Mineral genesis

The Juno deposit at Tennant Creek is made up of two separate bodies of magnetite enclosed within sediments of lower Proterozoic age. The ore elements are vertically zoned within these ellipsoidal magnetite-rich ore bodies (Large, 1974); gold is concentrated at the base, followed upwards by the bismuth sulphosalts and chalcopyrite. The further zoning of sulphosalts within the bismuth-rich portions is illustrated in Figure 5, with the lead-rich sulphosalts concentrated at the base of the ore body within the gold-rich zone. Passing upwards through this bismuth-rich zone to the copper ore, the lead content and the selenium content of the sulphosalts decrease, while the copper content increases (Large and Mumme, 1975).

Members of the bismuthinite–aikinite series beyond krupkaite (Mumme, 1975b) have not been observed in the mine. Junoite and proudite have formed in place of the known copper- (and lead-) rich members of this mineral series—lindströmite ($Cu_3Pb_3Bi_7S_{15}$), hammarite ($Cu_2Pb_2Bi_4S_9$), and aikinite ($CuPbBiS_3$)—due to a combination of the deficiency of copper and the excess of selenium passing towards the core.

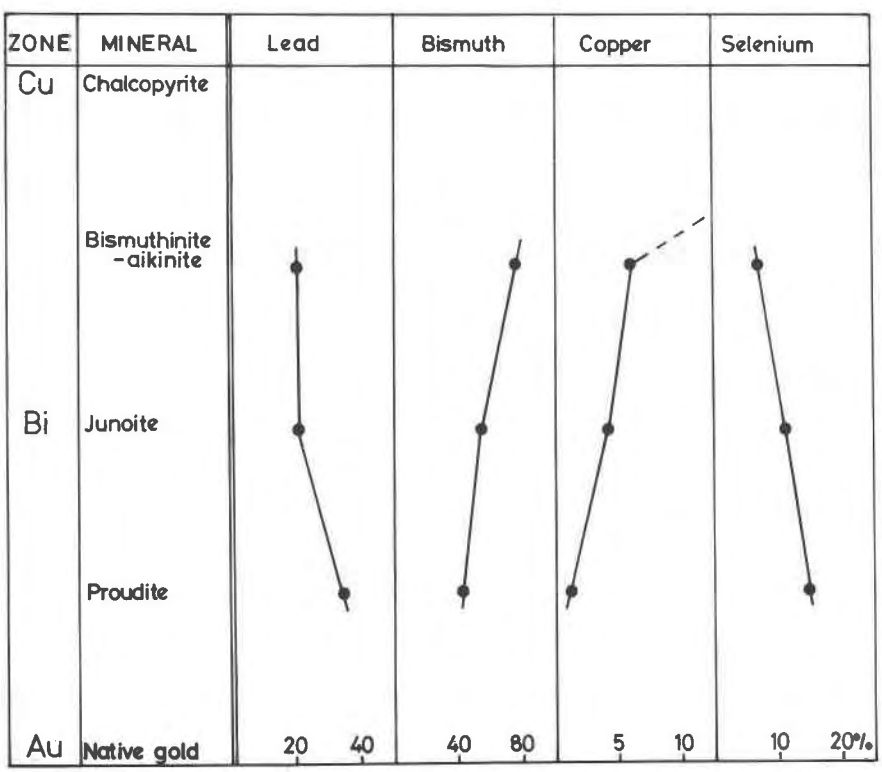

FIG. 5. Zonal relationships within the bismuth-rich portion of the Juno Mine.

The widespread presence of similar ironstone bodies is one of the outstanding features of the Tennant Creek field. It has been suggested that they formed as replacement bodies (Elliston, 1960) at relatively low temperatures (Wright, 1965) and that the emplacement of the magnetite was essentially completed before any introduction of gold, sulphide, and sulphosalt minerals into them (Edwards, 1955; Crohn, 1965). It would appear that the gold and bismuth in the Juno Mine belong to a late stage of the mineralization sequence, as is also suggested for the sulphide mineralization in the Orlando Mine at Tennant Creek (McNeil, 1966). A low temperature of formation is consistent with the fact that selenides mainly form during hydrothermal processes apparently at relatively low temperatures. Attempts have been made to synthesize proudite during studies in the $Bi_2(S,Se)_3$–Pb(S,Se)–$Cu_2(S,Se)$ system carried out at 500°C, but as in the case of junoite, without success. Again, it is unlikely that selenium-free varieties of proudite are stable in the Bi_2S_3–PbS–Cu_2S systems, as it appears that selenium is an essential component of the crystal structure and has become ordered during the relatively slow cooling process which has occurred after deposition.

References

Atteberg, A. (1874) Om ett selenhaltigt mineral från Falun grufva. *Geol. Fören. Förh.* **2,** 76–78.

Babkin, P. A. (1958) O nekotorykh selenovykh i selenosoderzhashchikh mineralakh (Some selenium minerals and selenium-bearing minerals). *Mater. Geol. Polez. Iskop. Sev.-Vostoka Evr. Chasti SSSR,* No. 13, 122–129.

Berry, L. G. and R. M. Thompson (1962) X-ray powder data for ore minerals. *Geol. Soc. Am. Mem.* **85,** 279p.

Busing, W. R., K. O. Martin and H. A. Levy (1962) ORFLS, a Fortran crystallographic least-squares program. *U.S. Natl. Tech. Inf. Serv.* ORNL-TM-**305.**

Crohn, P. W. (1965) Tennant Creek gold and copper field. In, J. McAndrew, Ed., *Geology of Australian Ore Deposits.* Melbourne, Australasian Institute of Mining and Metallurgy, 176–182.

Cromer, D. T. and J. T. Waber (1965) Scattering factors computed from relativistic Dirac-Slater wave functions. *Acta Crystallogr.* **18,** 104–109.

Cruickshank, D. W. J., D. E. Pilling, A. Bujosa, F. M. Lovell and M. R. Truter (1961). *Computing Methods and the Phase Problem in X-ray Crystal Analysis.* Oxford, Pergamon Press.

Earley, J. W. (1950) Description and synthesis of the selenide minerals. *Am. Mineral.* **35,** 337–364.

Edwards, A. B. (1955) The composition of the Peko copper ore body, Tennant Creek. *Australasian Inst. Min. Metall. Proc.* No. 172, 65–79.

Elliston, J. (1960) Ore localization by preconsolidation structures. *Australasian Inst. Min. Metall. Proc.* No. 196, 29–49.

Flink, G. (1910) Bidrag till Sveriges mineralogi. *Ark. Kemi Mineral. Geol.* **3,** No. 35, 5–7.

Grip, E. and Wirstam, A. (1970) The Boliden sulphide deposit: A review of geo-investigations carried out during the lifetime of the Boliden Mine, Sweden (1924–1967). *Sveriges Geol. Unders., Ser. C,* No. 651.

Hellner, E. (1958) A structural scheme for sulphide minerals. *J. Geol.* **66,** 503–525.

Johansson K. (1924) Ett par selenförande mineral från Falu gruva. *Ark. Kemi Mineral. Geol.* **9,** No. 9, 1–7.

Karup-Møller, S. (1970a) Weibullite, laitakarite, and bismuthinite from Falun, Sweden. *Geol. Fören. Förh.* **92,** 181–187.

——— (1970b) Gustavite, a new sulphosalt mineral from Greenland. *Can. Mineral.* **10,** 173–190.

Kato, A. (1959) Ikunolite, a new bismuth mineral from the Ikuno Mine, Japan. *Mineral. J. (Tokyo),* **2,** 397–407.

Kohatsu, I. and B. J. Wuensch (1973) The crystal structure of nuffieldite, $Pb_2Cu(Pb,Bi)\ Bi_2S_7$. *Z. Kristallogr.* **138,** 343–365.

Large, R. R. (1974) *Gold, bismuth, copper mineralization in the Tennant Creek District, Central Australia.* Unpublished Ph.D. Thesis, University of New England, N.S.W., Australia.

——— and W. G. Mumme (1975) Junoite, "wittite" and related seleniferous bismuth sulfosalts from Juno Mine, Northern Territory, Australia. *Econ. Geol.* **70,** 369–383.

McNeil, R. D. (1966) Geology of the Orlando Mine, Tennant Creek, Australia. *Econ. Geol.* **61,** 221–242.

Mumme, W. G. (1975a) Junoite, $Cu_2Pb_3Bi_8(S,Se)_{16}$, a new sulphosalt from Tennant Creek, Australia: its crystal structure and relationship with other bismuth sulphosalts. *Am. Mineral.* **60,** 548–558.

——— (1975b) The crystal structure of krupkaite, $CuPbBi_3S_6$, from the Juno Mine at Tennant Creek, Northern Territory, Australia. *Am. Mineral.* **60,** 300–308.

——— E. Welin and B. J. Wuensch (1976) Crystal chemistry and proposed nomenclature for sulphosalts intermediate in the system bismuthinite–aikinite (Bi_2S_3–$CuPbBiS_3$). *Am. Mineral.* **61,** 15–20.

Nordström, T. (1874) Mineralytiska bidrag. 2. Selenhaltigt mineral från Falun. *Geol. Fören. Förh.* **2,** 268–269.

Ödman, O. H. (1941) Geology and ores of the Boliden deposit, Sweden. *Sveriges Geol. Unders., Ser. C.,* No. 438.

Ontoev, D. O., N. V. Troneva, A. L. Tsepin, L. N. Vyal'sov and G. V. Basova (1972) Serebrasoderzhashchii vittit iz Vostochnago Zabaikal'ya (Argentiferous wittite from eastern Trans-Baikal). *Zap. Vses. Mineral. Obshchestv.* **101,** 476–480.

Peacock, M. A. and L. G. Berry (1940) Roentgenographic observations on ore minerals. *Univ. Toronto Stud. Geol. Ser.* **44,** 48–69.

Povarennykh, A. S. (1972) Crystal Chemical Classification of Minerals. New York, Plenum Press.

Sindeeva, N. D. (1964) *Mineralogy and Types of Deposits of Selenium and Tellurium.* New York, Interscience.

Srikrishnan, T. and W. Nowacki (1974) A redetermination of the crystal structure of cosalite. *Z. Kristallogr.* **140,** 114–136.

Strunz, H. (1957) *Mineralogische Tabellen,* third edition. Leipzig, Akademische Verlagsgesellschaft.

Takeuchi, Y. and R. Sadanaga (1969) Structural principles and classification of sulphosalts. *Z. Kristallogr.* **130,** 346–368.

———, J. Takagi and T. Yamanaka (1974) Structural characterization of the high-temperature phase *V* on the PbS–Bi_2S_3 join. *Z. Kristallogr.* **140,** 249–272.

Vlasov, K. A., ed. (1964) *Geochemistry and Mineralogy of Rare Elements and Genetic Types of Their Deposits.* Vol. II. *Mineralogy of Rare Elements.* Moscow, Nauka Publishing House.

VORMA, A. (1960) Laitakarite, a new Bi–Se mineral. *Bull. Comm. Geol. Finlande,* **188,** 1–10.

WEIBULL, M. (1885) Om selenhaltig galenobismutit från Falun grufva. *Geol. Foren. Förh.* **7,** 657–666.

WICKMAN, F. E. (1948) From the notes of the late K. Johansson. III. Galenobismutite and weibullite. *Geol. Foren. Förh.* **70,** 488–489.

WRIGHT, K. (1965) Copper ore deposit of the Peko Mine, Tennant Creek. In, J. McAndrew, Ed., *Geology of Australian Ore Deposits.* Melbourne, Australasian Institute of Mining and Metallurgy, 183–185.

Manuscript received, September 29, 1975; accepted for publication, January 13, 1976.